Physics 111B: Optical Pumping Report

Susanna Weber
Lab Partner: Shreya Nagpal

Abstract

The purpose of this lab is to demonstrate the use of optical pumping to drive an atomic Rubidium gas into a polarized state and subsequently determine the frequencies at which we can observe the splitting between atomic states known as the Zeeman interaction. We "pump up" a Rubidium atomic gas in order to spin polarize it, and use two coils in the Helmholtz configuration to create an RF field to drive transitions between Zeeman states. Using this set up, we determine the the nuclear spin of two isotopes of Rubidium as well as calculating the earth's magnetic field.

1 Introduction

Our objective in this lab is to observe transitions between Zeeman energy levels in two isotopes of Rubidium and record the frequencies at which these transitions occur when the atoms are excited by a magnetic field. In order to detect these changes in state, the atoms must be prepared in a spin polarized state, specifically so that the proportion of atoms in the initial state is much higher than those in the final state.

The method to spin polarize the gas is known as optical pumping. This occurs by exposing the atoms to circularly polarized infrared light with a spectrum that can drive transitions, and driving the gas into the highest energy state, at which point it will no longer absorb light.

Two electromagnetic coils are used to generate the radio-frequency (RF) magnetic field, which drives Zeeman transitions in the Rubidium energy levels. The field drives the atoms out of their pumped state, meaning the atoms in the gas absorb light once again. These changes in gas transparency can be detected by a photodiode, and using this apparatus in conjunction with an oscilloscope, we are able to determine the Zeeman resonant frequency by varying the current through a set of Helmholtz coils.

Using our measurements of the magnetic resonance frequency at different currents, we can determine the nuclear spins of the two Rubidium atoms in our set up. Furthermore, using these nuclear spins, we can make a measurement of the Earth's magnetic field. Our results agree with known values, demonstrating that our set up can function both as a probe of atomic structure and a magnetometer for very small magnetic fields.

2 Background

Rubidium atoms contain three forms of angular momenta, L, S, and I, which are also known as the angular quantum number, the spin angular momentum, and the nuclear spin, respectively. The angular momentum states are not degenerate, but rather, split into distinct energy levels, known as corrections, which are orders of magnitude smaller than the atomic energy. These corrections are known as the fine, hyperfine, and Zeeman interactions, with energy levels labeled J, F, and m_F respectively. A visualization of the energy splitting can be seen in Figure **??**.

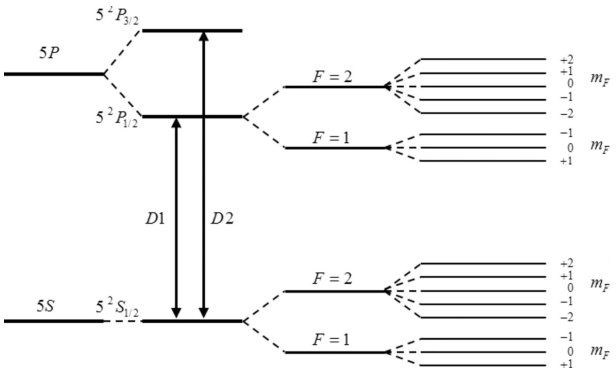

Figure 1: Energy levels of a Rubidium atom, showing fine, hyperfine, and Zeeman splitting. In this lab we are interested in the m energy levels, where the splitting is caused by applying a magnetic field. Source: [1].

In this lab, we are interested in what is known as the Zeeman effect, the transition of atoms between m_F states when exposed to a magnetic field. In the absence of a field, the magnetic moment of the atoms are randomly oriented, and the energy levels are degenerate. When a field is applied, however, the m_F energy levels split.

An important experimental caveat is that the magnetic field is equally likely to drive transitions from low to high or high to low m_F states. Thus, for a gas in an initially random mix of energy states, there will be no observable effect. In order to determine whether Zeeman splitting has occurred, we must first spin polarize the gas using optical pumping. The gas is exposed to circularly polarized light, which can drive transitions between m_F states. When the excited state decays, the atom releases a photon, and the quantum number changes by +1, -1, or 0. After each cycle, more and more atoms accumulate in the highest possible m_F state, until the gas is fully pumped. In this stage, the gas is no longer absorbing light. When the B field is applied, and the m_F energy levels change, the photons can be absorbed by the Rb atoms again. These changes in light intensity can be seen experimentally, making it

possible to observe Zeeman transitions. Specifically, we observe this effect at magnetic resonance.

This resonant Zeeman frequency can be derived using perturbation theory. We know

$$E = H\nu = g_F \mu_B B \tag{1}$$

where

$$g_F = g_J \frac{F(F+1) + J(J+1) - I(I+1)}{2F(F+1)},$$

$$g_J = 1 + \frac{J(J+1) + S(S+1) - L(L+1)}{2J(J+1)}$$

Using the known atomic numbers for Rubidium, $J = \frac{1}{2}$, $S = \frac{1}{2}$, L = 0, and F = 0, we can derive the Breit-Rabi formula, which relates the resonance frequency to the external magnetic field and the nuclear spin of the atom:

$$\frac{\nu}{B_{ext}} = \frac{2.799}{2I+1} \frac{MHz}{G}, \tag{2}$$

where ν is the resonant frequency, B_{ext} is the external magnetic field, and I is the nuclear spin [1]. B_{ext} is produced by the set of Helmholtz coils used in our experiment and the earth's magnetic field. In the case of a forward current through the coils, these two fields are summed, for a reverse current they are subtracted. The magnetic field produced by the coils can be found using the Helmholtz equation:

$$B_H = 0.9 \times 10^{-2} \frac{Ni}{a} \frac{Gm}{A} \tag{3}$$

Here, N is the number of coils, a is the the radius of the coils, and i is the current. Using equations 2 and 3, we can establish a relationship between the Zeeman resonance frequency ν and the applied current i.

3 Methods

3.1 Instrumentation

The atomic vapor consisting of Rb_{87} and Rb_{85} is contained in a glass bulb inside of a closed metal box to isolate it from any light sources. It is heated, in order to prevent it from settling on the sides of the bulb at a lower density, as this would make it difficult to observe changes in the transparency of the gas. The optical pumping light is generated by a lamp that can drive transitions from the Rb ground state. The light first passes through a circular polarizer, and then through a band-pass filter. This ensures that it can only drive the transitions that we are interested in observing. The light shines through the glass bulb containing the Rubidium and onto a photodiode connected to an amplifier. This output is then measured on an oscilloscope.

The box containing the atomic vapor and light is positioned between two electromagnet coils in the Helmholtz configuration. We use a function generator to send a sinusoidal signal through the coils and produce a magnetic field, which, due to the alignment of the coils, is parallel to earth's magnetic field. The field contains both a DC and an AC component. The AC signal is sent to the oscilloscope, which allows us to detect resonance by inspection. The DC signal is what controls the Zeeman resonance frequency we observe, and is what we vary in this experiment. We measure this DC component by measuring the voltage drop across a shunt resistor. A schematic of this experimental set up can be seen in Figure 3.1.

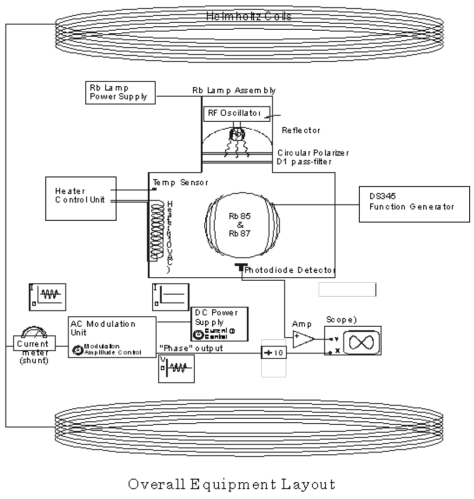

Figure 2: Diagram of our experimental set up. Source: [1]

3.2 Procedures

Using the set up described in the previous section, we apply a DC magnetic field to the vapor cell, inciting the Zeeman splitting. We use the function generator to output a sinusoidal current with a linear sweep of frequencies. We set the oscilloscope up in X-Y view in order to view the photodiode signal vs. the frequency of the field. Through this procedure we can observe the characteristic peak of optically detected magnetic resonance (ODMR) at the Zeeman resonance. Since we have two isotopes, we in fact observe a larger and a smaller peak, one for each isotope, with the height corresponding to the frequency of the isotope.

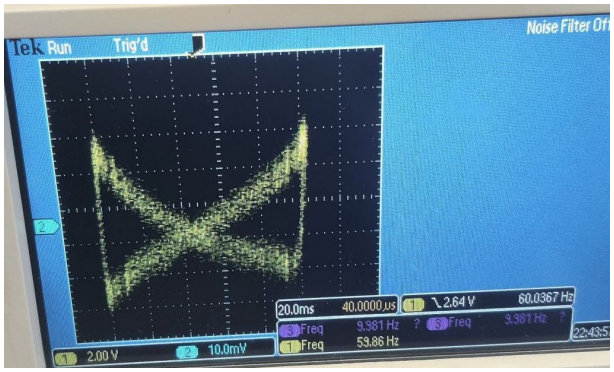

Figure 3: An example of Lissajous curve on a digital scope.

The second, and more accurate, approach that we pursue in order to detect the Zeeman resonance is modulating the Helmholtz current while applying a single-frequency magnetic field. We turn on field modulation in order to apply a 60 Hz modulation frequency to the Helmholtz coils, and then measure the variation of the measured signal at the modulation frequency. We plot this on the x-axis of our oscilloscope, and plot the photodiode voltage on the y-axis. We can now detect resonance by visual inspection - we scan the modulation frequencies, and at resonance, observe a symmetrical Lissajous curve on the oscilloscope. We take measurements at seven different current values, and at their inverse, in order to take data for both forward and reverse current through the coils. At each current, we took four separate measurements of the frequency at which we observed the symmetrical Lissajou curve, then averaged these to give us a value. At each current value, we observe resonances at two distinct frequencies, each one corresponding to the resonance observed at the Zeeman transition frequency for one of our two isotopes.

4 Results

Analysis Part 1 and 2 here In Figures 4 and 4, we plot the resonance frequencies as a function of the DC current that was sent through the coils, for both forward and reversed currents and both ^{85}Rb and ^{87}Rb. We first perform a weighted fit by writing a function that performs the standard linear regression procedures described in REF HERE in order to find the slope and intercept, as well as their errors, for a line of best fit to both forward and reversed currents. To calculate the weight of each data point, we used the standard error, $\frac{\sigma}{\sqrt{N}}$. Here, σ is the standard deviation of the four frequency measurements taken at each current, and correspondingly, N = 4. These weights are also plotted as linear error bars in Figures 4 and 4 but they are too small to be seen on the MHz y-axis scale. We then performed an unweighted fit using the scipy.optimize.curvefit function in Python and the square of the summed residuals as our error.

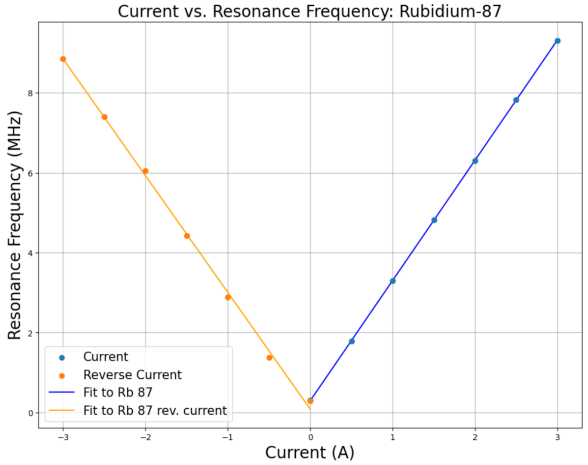

Figure 4: Weighted fit to observed ^{87}Rb Zeeman resonance frequencies, measured at seven forward current and seven reversed current values. Error bars are too small to be seen on MHz y-scaling.

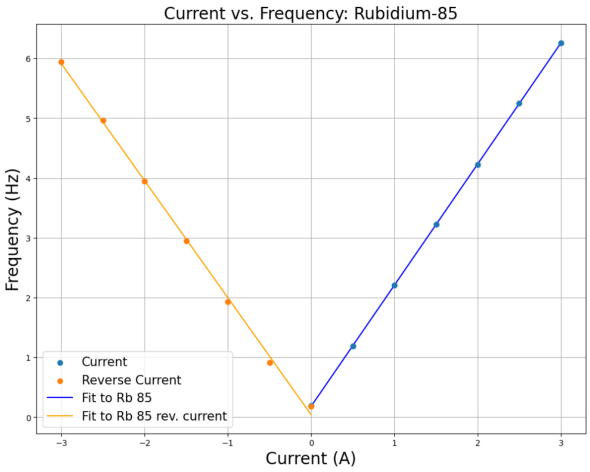

Figure 5: Weighted fit to observed ^{85}Rb Zeeman resonance frequencies, measured at seven forward current and seven reversed current values. Error bars are too small to be seen on MHz y-scaling.

The fitted and unfitted parameters and their errors can be found in Table 1, which also contains the chi squared values for these fits. The fits for our forward current give us chi squared values with p values slightly less than 0.01, indicating that we have an appropriate fit. For our reversed currents, however, we get unreasonably large chi squared, which, while showing our fit is appropriate, is indicative of data that is "too good to be true" [3]. We believe that this has happened because we were using a digital scope for our Lissajous curves, which produced very fuzzy results. This low-resolution made it very difficult for us to observe a range of frequency values at which we observe resonance, meaning that our standard deviation, and correspondingly our errors, are very small. This produces a very large chi squared, making it a poor metric this data. By visual inspection of the fit, and the fact that our fitted values agree for both weighted and unweighted fits, are indicative of a good fit.

After performing these fits, we plotted the current and reverse current data on one line for each isotope by making the frequencies observed at negative currents negative as well. The data was fitted using a weighted linear regression. Fitting parameters and errors are shown in Table 1. We fit these data using the same linear regression function from earlier. Again, we have unreasonably large ξ^2 values due to our small standard distributions. By inspection, and the close match with our fits for the previous two graphs, we can see that our fit is a close match to the data. Standard errors were used to produce error bars on the plot, but are too small to be seen with the y-axis scaling. We continue to use the parameters found in these fits for our data analysis since they are based on more data points and should therefore be more reliable.

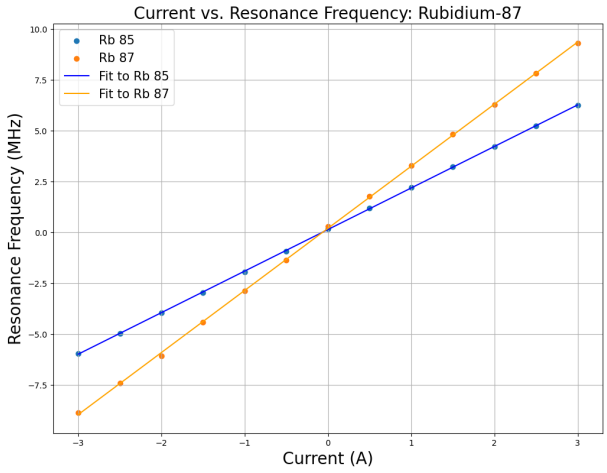

Figure 6: Fit to resonance frequencies at fourteen different current measurements for ^{87}Rb and ^{85}Rb. Forward and reverse current measurements were plotted on a line by negating the frequency measurements taken at reversed currents.

5 Analysis

5.1 Determining Nuclear Moments

Using our current-vs frequency data, we use two methods to determine the nuclear sp ins of the two Rb isotopes, I_85 and I_87. First, we plot the resonance frequencies for ^{87}Rb against ^{85}Rb and determine the slope and intercept using a linear regression fit. We find that that the slope, $m_{/nu}$ is 1.486 ± 0.02, and the intercept,$b_{/nu}$ is 0.02 ± 0.008.Through algebraic manipulation of Equation 2, and combining the expression for both the ^{87}Rb against ^{85}Rb case, we find that

$$\frac{\nu_{87}}{\nu_{85}} = \frac{B_{ext,87}}{B_{ext,85}} \frac{2I_{85}+1}{2I_{87}+1} \tag{4}$$

In this case, since our currents are equal for each point, our B-fields produced by the Helmholtz coils will also be equal, and thus the B_{ext} term is equal to one. The known values of I_{87} and I_{85} are $\frac{3}{2}$ and $\frac{5}{2}$, respectively. Therefore, the expected value of $\frac{\nu_{87}}{\nu_{85}} = \frac{3}{2}$. Since our fitted intercept is extremely close to 0, we ignore it here and instead set:

$$\begin{aligned} \nu_{87} &= m_\nu \nu_{85} \\ \frac{\nu_{87}}{\nu_{85}} &= m_\nu \end{aligned} \tag{5}$$

Comparing this fitted slope to the expected value of 1.5, we find that the true value is within the error bounds of our our result. Thus, we have found an accurate estimate of the ratio of the nuclear spins of our two isotopes.

We now want to determine the individual nuclear spins. To do this, we again refer to Equation 2. Rearranging and plugging in Equation 3 for B_{ext}, the Breit-Rabi equation can be re-written as

$$\frac{v}{i} = \frac{2.799}{2I+1} \frac{0.9 \times 10^{-2} N}{a}, \tag{6}$$

where $N = 137$ is the number of loops in our Helmholtz coils and $a = 27.5cm$ is the radius of the coils. Note that here we are ignoring the ambient field produced by the earth for simplicity and since it is small compared to the field produced by the Helmholtz coils. Once again we can see that the right-hand side of our equation is equal to one of our fitted slopes, specifically, the fit shown in 4, where we plot the frequency as a function of current for all of our data points combined. Rearranging Equation 6 to solve for the nuclear spins, we find that $m_{85} = 2.57 \pm 0.145$ and $m_{87} = 1.55 \pm 0.205$. Both results agree with the theoretical values of $I_{85} = 2.5$ and $I_{87} = 1.5$, showing that our approximation of ignoring the Helmholtz field was valid, and that we can use our experimental set up as a probe of atomic properties.

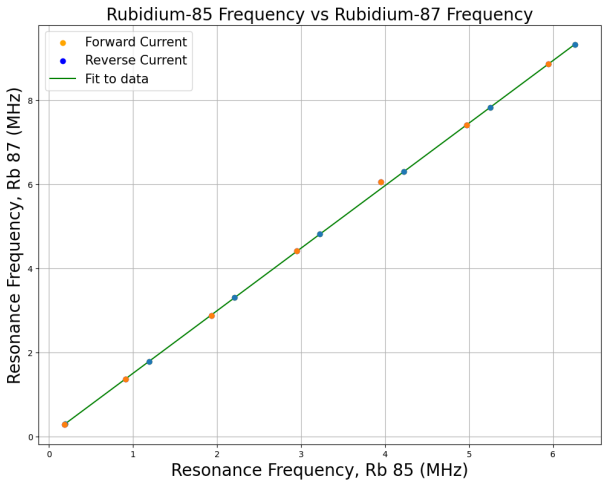

Figure 7: Resonant frequencies for ^{87}Rb plotted against resonant frequencies for ^{85}Rb, fitted using a non-weighted linear regression.

5.2 Measuring Earth's Magnetic Field

We can also use our set up as a magnetometer. We know that, apart from the field produced by the

Table 1: Slopes and intercepts for different fits to current vs frequency data.

Fit	Weighted?	Slope	Intercept (MHz)	χ^2
^{85}Rb, Fwd. Current	Y	2.02 ± 0.001	0.182 ± 0.002	18.32
^{85}Rb, Rev. Current	Y	-1.93 ± 0.003	0.084 ± 0.005	17.55
^{87}Rb, Fwd. Current	Y	3.01 ± 0.002	0.290 ± 0.004	607.4
^{87}Rb, Rev. Current	Y	-2.92 ± 0.004	0.096 ± 0.008	928.41
^{85}Rb, Fwd. Current	N	2.03 ± 0.003	0.181 ± 0.005	47.51
^{85}Rb, Rev. Current	N	-1.96 ± 0.033	0.042 ± 0.060	18.13
^{87}Rb, Fwd. Current	N	3.01 ± 0.002	0.290 ± 0.009	671.27
^{87}Rb, Rev. Current	N	-2.92 ± 0.050	0.083 ± 0.0980	1616.56
^{85}Rb, Combined	Y	2.042 ± 0.004	0.145 ± 0.007	412.00
^{87}Rb, Combined	Y	3.053 ± 0.010	0.203 ± 0.020	1095.70

Helmholtz coils, our set up is subject to the earth's magnetic field as well. We pursue two approaches.

First, we turned off the DC current being run through the Helmholtz coils, both in the forward current and reverse current setting, and noted at what frequency we observed resonance. Using Equation 2 we found the corresponding B_{ext}, which, at 0 DC current, is our measurement of the earth's magnetic field. Since we observed resonance for both isotopes, we arrived at two estimates.

Our second approach was to use the y-intercept from the fit in Figure 4. From Equation 3 we know that the Helmholtz magnetic field is zero at this point, and can plug the frequency into 2 to get the corresponding frequency. We can then calculate the earth's magnetic field using Equation 3. Since this calculation gives us the value of the field needed to cancel the ambient field, we negate our result to get an estimate of the earth's field. Results for both approaches can be found in Table 2.

Table 2: Calculations of Earth's magnetic field for two different approaches and two isotopes.

Approach	Isotope	Field (G)
1	^{85}Rb	0.41 ± 0.01
1	^{87}Rb	0.42 ± 0.01
2	^{85}Rb	0.41 ± 0.02
2	^{87}Rb	0.43 ± 0.03

The true value of the earth's magnetic field in Berkeley is 0.48 G [4]. Our calculated values agree with each other, but not the actual magnetic field. Some reasons for this could include that we were only measuring the magnetic field along one axis, giving us a less accurate result, and that other magnetic fields in the room may have affected our measured ambient field.

5.3 Resonance Observed at B = 0

We can use our result for the Earth's magnetic field to find that we observe resonance even when $B_{ext} = 0$. In order to achieve this, we turn off the RF field modulation altogether, and then scan the current. We can find the appropriate current value using the value of the earth's magnetic field and Equation 3. When the field being produced by running the current through the coils exactly cancels the Earth's magnetic field, we (strangely) still observe resonance at 0.9 A, corresponding to a B-field of $.39 \pm 0.046$ G. This occurs because, despite the fact that we are cancelling the field at the center of our set up, there are still edge-effects occurring further out from the center where the field is not cancelled. These effects produce the resonance that we observe even when we are trying to completely cancel out the earth's field.

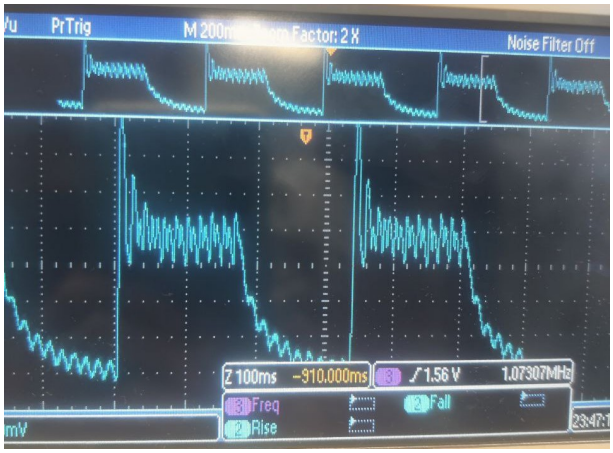

Figure 8: Photodiode signal when using a square wave modulation and a resonant frequency sine wave, displaying Rabi oscillations.

5.4 Timescales for Optical Pumping

In order to observe the "pumping time" and the relaxation time for our set up, we set the function generator to output an amplitude modulated sinusoidal signal, where the amplitude modulation is a square wave at 4 Hz and the sinusoidal signal is at a frequency at which we observed a particularly strong resonance. By observing the photodiode signal on the scope, we saw that when the field was off, the gas was optically pumped and transparent, meaning more light was reaching the photodiode, and when it was on, the gas became opaque as the atoms left the pumped state and we observed a smaller signal.

Figure 5.3 shows this effect, as well as Rabi oscillations. These are signal oscillations that occur

when a two-state system in a superposition evolves with time. Thus, we are observing oscillations due to the fact that we are in a superposition of being pumped and not pumped.

Since we were reading off of the scope by visual inspection rather than doing more thorough measurements, we did a series of of four inspections, in between which we turned the oscilloscope off. We determined the relaxation time to be $1.5 \times 10^{-6} \pm 2 \times 10^{-6}$. The error was determined using the standard error formula. As is visible in Figure 5.3, the pumping time was extremely fast, and we were unable to reliably determine it by inspection of the oscilloscope. Therefore, we restrict ourselves to stating that it is significantly less than the relaxation time.

Calculating the theoretical value to compare this to is a very involved process, so it was not a part of this lab. An extension of the analysis for this lab could be to find this value using Fermi's Golden Rule, which describes a system that begins in an eigenstate of a Hamiltonian and is then perturbed. The transition probability per unit of time from the initial state to the final state if given by:

$$\Gamma_{i \to f} = \frac{2\pi}{\hbar} |\langle f|H|i\rangle|^2 \rho(E_f), \tag{7}$$

where f is the final state, i is the initial state, H is the perturbing Hamiltonian, and ρE_f is the density of states ([5]). This term is called the decay probability and is related to the mean lifetime. Thus, a more detailed quantum mechanical understanding of the system would be required to experimentally determine this value.

6 Conclusion

In this experiment we used optical pumping to spin polarize a Rubidium gas consisting of two different Rb isotopes. Using an RF magnetic field to drive the atoms, we observed the resonance frequencies of the Zeeman splitting resulting from the applied field. We then analyzed our data in order to calculate the nuclear spin of both isotopes in the gas and estimate the earth's magnetic field. We have summarized different mathematical approaches to these tasks and compared them to known values, finding them to be in agreement for nuclear spin and on a very similar scale for the magnetic field.

7 Acknowledgements

Thank you to my lab partner, Shreya Nagpal, Professor Pyle, Professor Williams, and the 111B GSIs and tutors for their assistance with this lab.

8 References

1. Physics 111B: Advanced Experimentation Laboratory. *OPT - Optical Pumping.* University of California, Berkeley.
2. Li, Y., Wang, Z., Jin, S., Yuan, J., amp; Luo, H. (2017). *Elliptical polarization of near-resonant linearly polarized probe light in optically pumped alkali metal vapor.* Scientific Reports, 7(1).
3. Lyons, L. (1991). *A practical guide to data analysis for Physical Science Students.* Cambridge University Press.
4. NOAA. *Magnetic Field Calculators.* National Oceanic and Atmospheric Administration.
5. Wikimedia Foundation. (2022, September 30). *Fermi's golden rule.* Wikipedia.